STRENGTH OF SELF-PIERCING RIVETED JOINTS FOR CFRP/ALUMINIUM SHEETS

L. Kroll[1], S. Mueller[1,3]*, R. Mauermann[2], R. Gruetzner[2]
[1] Chemnitz University of Technology, Institute of Lightweight Structures, Chemnitz, Germany,
[2] Fraunhofer Institute for Machine Tools and Forming Technology, Dresden, Germany
[3] Lightweight Structures Engineering GmbH, Chemnitz, Germany
* Corresponding author (sascha.mueller@mb.tu-chemnitz.de)

Keywords: *joining, self-piercing rivet, CFRP, aluminium sheets*

1 Introduction

Multi material design in lightweight applications is most probable the challenging task in the future. Only the right material in the right place can exploit full use from the positive properties of each material. Under many environmental and economical points of view hybrid structures moved into the centre of the interest in different branches [1]. Joining technologies are essential for practical applications of hybrid materials and structures [2]. In particular, the automotive industry is looking for alternative materials and appropriate joining techniques [3–5]. Thereby, self-pierce riveting (SPR) offers a long list of advantages compared to more traditional methods of sheet material joining [6]. It is a fast and clean technique to join dissimilar materials with no need for pre-drilled holes. Although, SPR is inappropriate for brittle substrates, Fratini and Ruisi have shown that SPR can be used to join fibreglass composite panels and aluminium blanks if the composite laminates are placed at the top of the joint [7]. In this study, semi-tubular self-pierce riveting joints between carbon fibre reinforced laminates (T700SC/RIM935) and aluminium alloy sheets (AlMgSi0,5 T6) were investigated experimentally to study the mechanical behaviour in dependence of the fibre orientation. For a better understanding of the inward phenomena, finite element simulations have been carried out and have been verified by the experiments.

2 Self-piercing riveting process

SPR is being used more to join metal sheets and not to join brittle materials like composites with epoxy resin matrix. Nevertheless, the joining of CFRP laminates with aluminium sheets was obtained in this study by using a flat and round head rivet with an optimal yield strength and hardness by Böllhoff GmbH. When the yield strength of the self-piercing rivet material was too low, the self-piercing rivet was deformed before it could pierce the top CFRP laminate. If the yield strength of the self-piercing rivet material was too high, the self-piercing rivet could not deform, so it could not form an interlock with the aluminium sheet.

The process of setting a semi tubular rivet is divided in three steps (see Fig. 1.). In the first step the sheets had been fixed locally between the blank holder and the die before they were pierced by the rivet. Thereby the sheet on the die side is pierced only partial. Next, the flaring of the rivet is influenced by its own hardness, geometry, and material. Further, properties of the substrates as well as the tool geometry affect the flaring. In the last step the punch continues the stroke, pushing the rivet inside the aluminium sheet to be joined. The tools for the joining task in this paper were chosen by performing experimental and numerical investigations (Fig. 1 and Fig. 2) similar to [8].

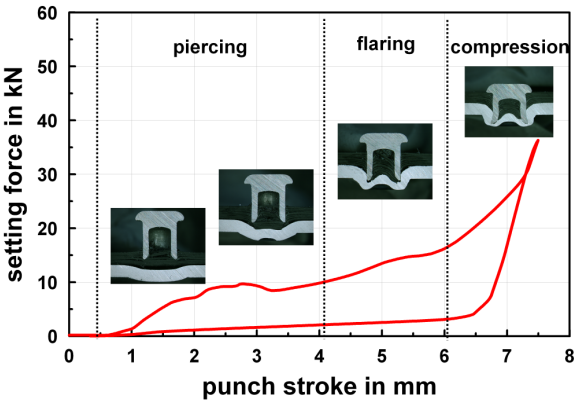

Fig. 1. Setting force vs. punch stroke curve with operational sequence of the SPR process.

The rotationally symmetric model aims at the determination of geometric quality criteria like

undercut, deformation of the rivet and forming force. It considers plastic material behaviour for the aluminium sheet and the tubular rivet while the fibre reinforced material is modelled purely elastic. To reduce the effort of the numerical model the element stiffness of elements exceeding the yield point is reduced. In spite of the chosen assumptions the comparison of simulative and experimental results (Fig. 2) is in accordance with geometric quality criteria. While the deformation of the rivet matches with the measurements in the micro section the simulation underestimates the deformation of the aluminium sheet in the area of the die.

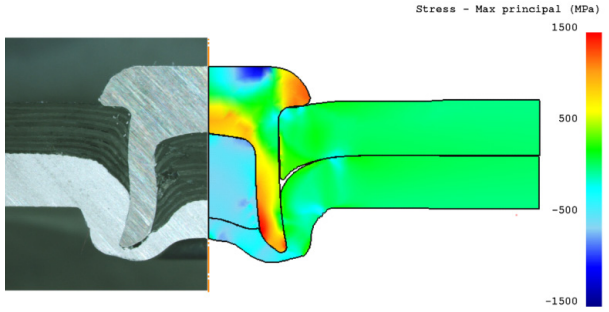

Fig. 2. Comparison between experimental and simulated section; right: micro section; left: max principal stress distribution at the end of the joining procedure (2D-model).

3 Micro section analyses

The micro-sectional view of a manufactured joint is shown in Fig. 3. Hereby a cross-ply-laminate with $[0/90]_{4S}$-layup and an extruded aluminium alloy sheet, both 2 mm in thickness, were joined point wise by SPR. The rivet was pushed through the top CFRP laminate into the bottom sheet. Then the aluminium sheet flew into the die and the rivet shank was flared in radial direction to form a mechanical interlock. This joint has no through-hole and therefore is impermeable to air and fluids; it is 'water tight'. In contrast formed bulges may not be acceptable regarding aesthetic aspects [6].

A close-up of the laminate structure is shown in Fig. 4. It can be observed that the punched core of the CFRP-laminate is strongly deformed and damaged. Due to the fact that the punched core remains in the semi-hollow shank, this joining technique produces no waste material and makes the riveting process clean.

The upper part of the core is excessively damaged. Fibre fracture as well as inter fibre fracture can be found in this region while the structure of the laminate is almost unrecognisable. The lower part of the core still reveals the laminate layup, but the former flat and plane layers are curved after the riveting process.

Fig. 3. Micro section of a semi tubular self-piercing rivet between a carbon fibre reinforced laminate ($[0/90]_{4S}$-layup) and an aluminium alloy sheet.

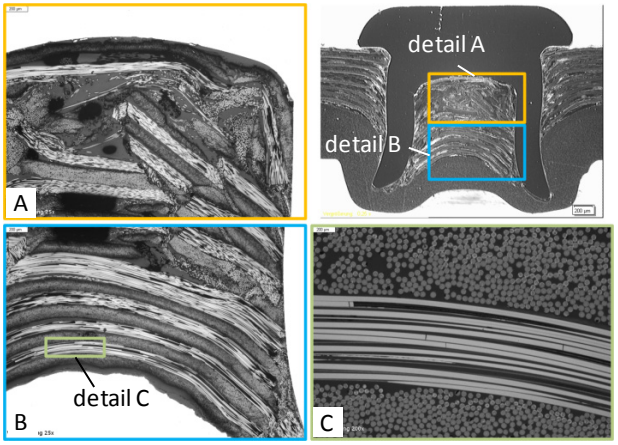

Fig. 4. Close-up of the deformed and damaged laminate structure inside the rivet shank.

In Fig. 5, the laminate structure outside of the rivet is depicted more precisely. All layers are curved in the direction of rivet setting. The curvature radius of the bottom layer is taller than the curvature radius of the top layer. Both, top and bottom layer, seem to be mostly undamaged while fibre fracture and delamination occur near the middle layers. The layers in 0°-orientation (brighter layers with fibres

running from left to right) were cut by the rivet. In the middle region, they are also broken in a characteristic distance to the rivet shank. Because of their fixed length, they leave the 0°-orientation. The layers in 90°-orientation (perpendicular to the micro section) are deformed without fibre fracture. These layers show a sort of shearing bands between the fibres. Although the matrix – made of epoxy resin – has a brittle behaviour, it shows no inter fibre fracture. Furthermore, it is assumed that the matrix becomes plastically deformable due to the high compression stress during the riveting process. This effect had already been observed [9].

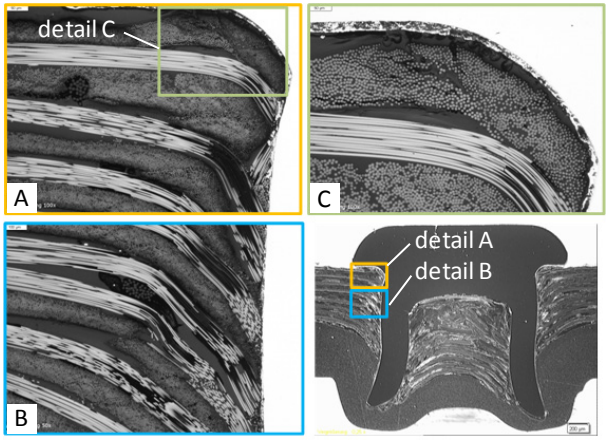

Fig. 5. Close-up of the deformed and damaged laminate structure near the rivet shank under the rivet head.

4 Mechanical behaviour of SPR joints

Many research studies are focused on comparisons of the mechanical behaviour of joints manufactured by various techniques; like spot welding, press joining, pop riveting, self-tapping screws, self-pierce riveting and more. A summary for metal materials is given by He et al. in [8]. In this study, the behaviour of SPR joints was investigated with focus on the CFRP composite by using single lap shear tests. The testing speed was set for all specimens at a displacement controlled quasi-static loading with 2 mm/min. The specimens have a gauge length of 95 mm and a width of 45 mm. The aluminium sheets as well as the CFRP laminates were 2 mm in thickness, and the rivet was placed at the centre of the 36-mm-long overlap (see Fig 6). The rivet dimensions are ∅5.3 mm x 5.6 mm with a head diameter of 7.7 mm.

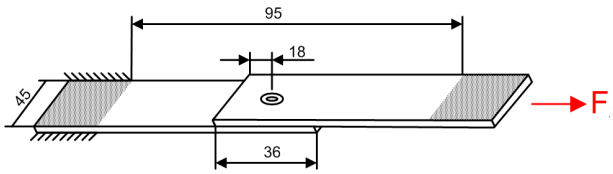

Fig. 6. Dimensions of the specimen.

To determine strength and fracture mechanisms in depending on different orientation angles φ, the tests were performed under φ = 0°, φ = 15°, φ = 30° and φ = 45° with cross-ply-laminates with a $[0/90]_{4S}$-layup. All other geometric, material and process parameters are constant in these tests.

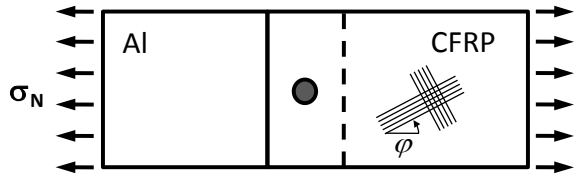

Fig. 7. Quasi-static test specimen with the cross-ply-laminate under φ = 0°, φ = 15°, φ = 30° and φ = 45° to the loading direction.

Load vs. displacement curves for quasi-static single lap shear tests (φ = 0°) are shown for five specimens in Fig. 8. The marked points A, B...E refer to the images in Fig. 9.

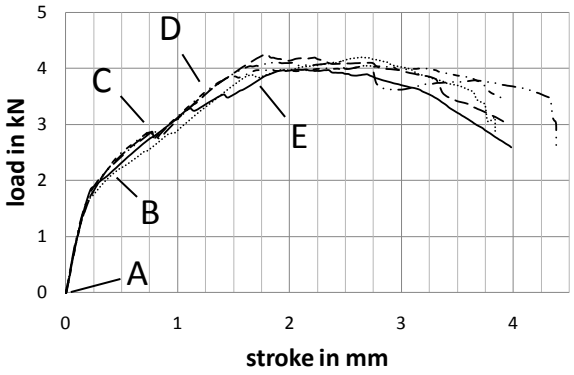

Fig. 8. Load vs. displacement curves for performed quasi-static single lap shear tests for φ = 0°.

These images of a lap shear test give a good impression of the complex mechanism of the joint specimen under loading. Beginning from the unloaded state A all specimens showed a reversible elastic behaviour up to 1.65 kN. Then the tip of the aluminium sheet has formed a gap and the rivet has begun to tilt (state B). At point C three of the five specimens showed a short break in their curves.

Here, at the load level of 2.7 kN and the stroke of 0.8 mm, the rivet head has penetrated the top CFRP laminate and the material of the lower sheet was dislodged due to the plastic deformation of the undercut near the rivet foot. The maximum strength of these tests is reached at 4.12 kN load (state E).

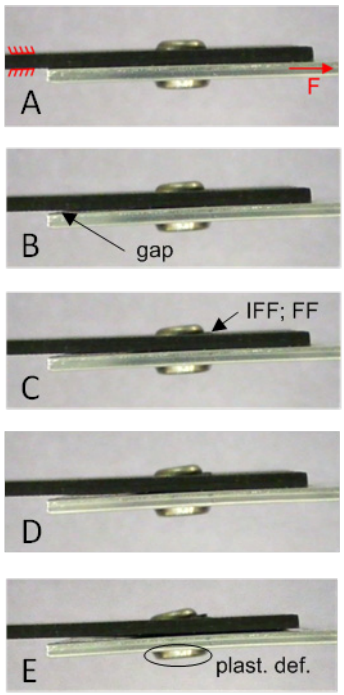

stroke Δs = 0 mm, unloaded specimen

Δs = 0.4 mm, rivet begins to tilt, tip of aluminium sheet forms a gap

Δs = 0.8 mm, rivet head penetrates the CFRP laminate

Δs = 1.2 mm, plastic deformation in the aluminium sheet

stroke Δs = 1.6 mm, joint is going to damage

Fig. 9. Image series taken of a single lap shear test.

The load vs. displacement curves for the specimens with laminate orientation of φ = 0°, 15°, 30° and 45° are shown in Fig. 10.

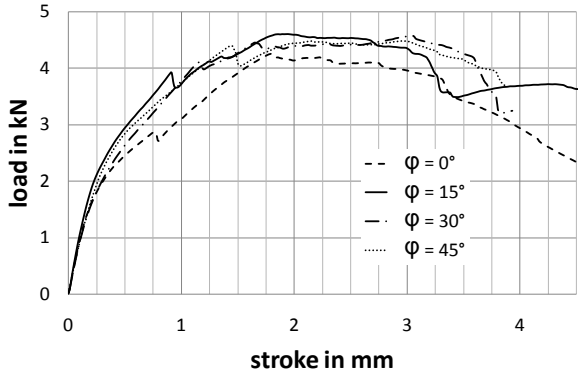

Fig. 10. Load vs. displacement curves for single lap shear tests with different laminate orientation.

In this diagram, one representative curve for each orientation angle φ was chosen from five tests for φ = 0° and from three tests for each other angle. It has to be mentioned that all curves show only a low scattering and no test must been withdrawn. Although a cross-ply laminate has elastic properties which are strongly dependent on the loading direction, the load vs. displacements curves are very similar for all chosen angles φ (Fig. 10).

The maximum load and the corresponding stroke are summarised for all specimens in Table 1. It can be seen that the specimens with φ = 0° orientation induce the lowest strength of the investigated joints. Due to the highest stiffness in loading direction it is assumed that the rivet was driven to tilt under a lower load than the other specimens do. These specimens show no significant difference regarding the maximum force.

specimen	orientation angle	maximum force in N	stroke at max. force in mm
1	φ = 0°	4248.41	1.79
2	φ = 0°	4122.08	2.46
3	φ = 0°	4051.12	2.69
4	φ = 0°	4198.78	2.66
5	φ = 0°	3981.39	2.15
6	φ = 15°	4599.14	1.94
7	φ = 15°	4630.60	2.30
8	φ = 15°	4616.13	1.49
9	φ = 30°	4569.25	3.05
10	φ = 30°	4505.75	2.14
11	φ = 30°	4438.62	2.65
12	φ = 45°	4488.49	2.96
13	φ = 45°	4752.92	2.36
14	φ = 45°	4684.46	1.64

Tab. 1. Maximum load and corresponding stroke in dependence of fibre orientation of $[0/90]_{4S}$-laminate.

The strength of SPR joints is governed by two principle fracture mechanisms: i) deformation of the bottom aluminium alloy sheet and ii) penetration of the rivet head into the top CFRP laminate. Both effects are depicted in Fig. 11. The rivet is more stiff than the sheets and applies a compressive force which leads to a damage in the contact area to the CFRP laminate as well as to a plastic deformation of the aluminium alloy sheet. The tilting of the rivet was favoured by the deformation of the aluminium sheet. That increased the resulting moment before the rivet head was cutting himself into the top CFRP laminate.

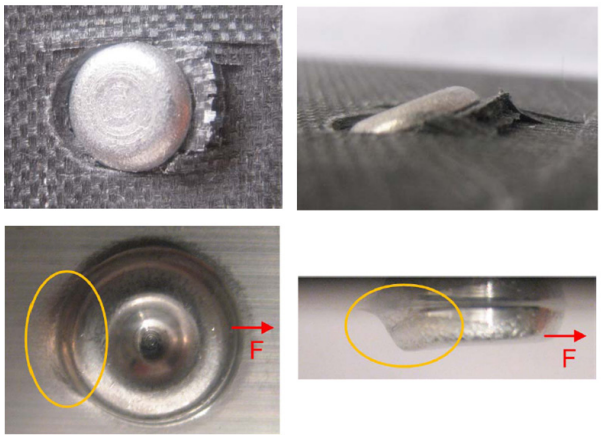

Fig. 11. Plastic deformation of the bottom aluminium alloy sheet leads to a tilting rivet and thus to a brittle damage of the upper CFRP laminate.

5 Finite element analysis

A 3D finite element model of the joint formation has been established by taking a contour drawing from a micro section, which then was rotated in CAD software to create a volume model. The associated mesh is shown in Fig. 12.

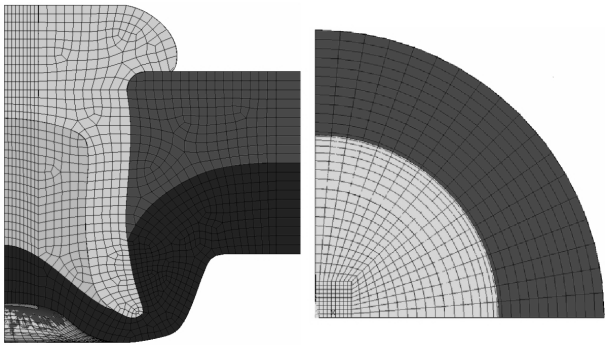

Fig. 12. FE mesh of semi-tubular self-piercing riveted joints for CFRP/aluminium sheets.

The model has been created in ANSYS 12.1 with the elastic anisotropic properties of CFRP, the elastic-plastic behaviour of the aluminium and geometric non-linearity in mind. The CFRP cross-ply laminate is described with smeared parameters determined with the classical laminate theory. The material parameters used for the simulation were all taken from databases and literature. They are summarised in Tab 2. The validation of the model has been carried out by comparison of the numerical results with experimental ones.

parameter	value
E_x	62.28 GPa
E_y	62.28 GPa
E_z	7.0 GPa
G_{xy}	2.8 GPa
G_{xz}	2.3 GPa
G_{yz}	2.3 GPa
ν_{xy}	0.035
ν_{xz}	0.31
ν_{yz}	0.31

parameter	value
E_{rivet}	210 GPa
ν_{rivet}	0.3

parameter	value
E_{al}	70 GPa
ν_{al}	0.34

stress in MPa	plastic strain
70	0.000
204	0.002
213	0.005
229	0.030
247	0.068
255	0.095
255	2.000

Tab. 2. Material properties used in simulation; left: smeared anisotropic parameters of CFRP cross-ply laminate and elastic parameters of the rivet; right: elastic and plastic properties of AlMgSi0,5 T6.

In this investigation the total joint force is transmitted through a single rivet while no by-pass loading occurs. Therefore, the contact zone to the rivet carries very high compression loads which lead to a plastic deformation of the aluminium sheet. The plastic work of the aluminium sheet is shown in Fig. 13. Due to the direction of loading the maximum plastic deformation is here on the left side. This plastic deformation corresponds to the observation in the experiments (cp. Fig. 11). The aluminium sheet opens the closure in this region and allows the rivet to tilt. Furthermore, a second concentration of the plastic work can be seen laterally – almost perpendicular to the loading direction. This local maximum is caused by the opposite side of the rivet, which tries to come off the undercut, and the affecting tensile load. Incidentally, this point is often the starting point of the crack formation in fatigue tests.

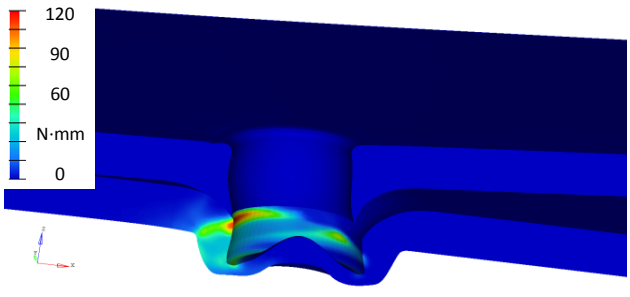

Fig. 13. Plastic work of the aluminium sheet.

The deformed contour plot of the investigated self-piercing riveted joint is shown in Fig. 14. Many possible contact pairs are forming gaps, while four distinct contact areas can be identified between: i) rivet head and CFRP laminate, ii) rivet shank and CFRP laminate, iii) rivet foot and aluminium sheet on compression side, and iv) rivet foot and aluminium sheet on supporting side. The deformed shape of the model does not match to the observed shape in the experiments. This is mainly attributed to contact pairs ii). The laminate near the rivet shank had been damaged during the setting process (cp. Fig. 4) before the joint came in use. The degraded material properties of the CFRP laminated in this region were not taken into account because they are almost impossible to determine.

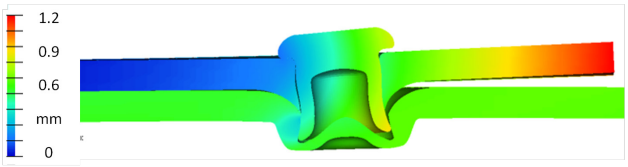

Fig. 14. Deformation of semi tubular self-piercing riveted joints for CFRP/aluminium sheets.

The stress in z-direction is of particular interest because the rivet head tilts and therefore cuts himself into the top CFRP laminate. Fig. 15 shows this high compression occurring in this region. Due to some simplified assumptions the value is some order too high, but the damage inducing point in the joints formation can be identified in this simulation.

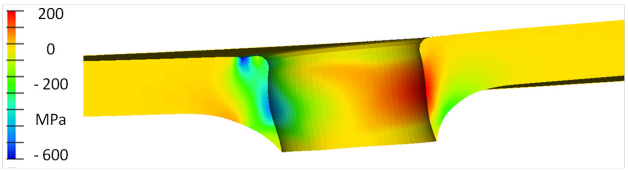

Fig. 15. Stress in z-direction (laminate thickness).

4 Conclusions

This study demonstrates that SPR can be used effectively to join CFRP laminates and aluminium sheets. Thereby, a high reproducibility of this joining process was achieved. The micro section analyses show that the laminate structure is damaged in different regions which are not the point of the latter joint failure. Further, the laminate orientation φ has only a slight influence on the strength of the joint, while the orientation φ = 0° shows the lowest maximum force. Therefore, the orientation of the laminate is not significant in the designing process. The FE simulation takes anisotropic mechanical properties and non-linearities such as material plasticity and contact among deformable parts into account. Damage and facture were neglected in this study. Hence, the quantity of the numerical results is inaccurate, but the failure mechanisms have been identified. The plastic deformation of the bulges in the aluminium sheets and compression stress under the rivet head in laminate thickness lead to a tilted rivet and cause the joint failure.

Acknowledgements

The authors gratefully acknowledge the financial support of this research by Deutsche Forschungsgemeinschaft and Arbeitsgemeinschaft industrieller Forschungsvereinigungen within the DFG-AiF-Cluster “KOMMA”.

References

[1] “*The worldwide composites industry: Structure, Trends and Innovation*”, JEC Publications, 2010.

[2] Kroll, L., Czech, A., Ulke, L., Mueller, S., “Mechanical behaviour of bolted joints with load adapted fibre orientation by variabel-axial fibre placement”. *16th Int. Conf. on Mech. of Comp. Mat.*, Riga, 2010.

[3] Hahn, O., Neugebauer, R., Leuschen, G., Kraus, C. and Mauermann, R. “Research in impulse joining of self pierce riveting”. *High Speed Forming 2008: 3rd Int. Conf. on High Speed Forming*, 2008.

[4] Carle, D., Blount, G. “The suitability of aluminium as an alternative material for car bodies”. *Mater. Design* 20, 267–272, 1999.

[5] Barnes, T.A., Pashby, I.R. “Joining techniques for aluminum spaceframes used in automobiles. Part II – adhesive bonding and mechanical fasteners”. *J. Mat. Processing Technology*, 99 (1), pp. 72–79, 2000.

[6] He, X., Pearson, I., Young, K. “Self-pierce riveting for sheet materials: State of the art”. Journal of Materials Processing Technology, Vol. 199, pp 27–36, 2008.

[7] Fratini, L., Ruisi, V.F. “Self-piercing riveting for aluminium alloys-composites hybrid joints”. *Int. J. Adv. Man. Technology*, 43 (1-2), pp. 61-66, 2009.

[8] Atzeni, E., Ippolito, R., Settineri, L. “FEM modeling of self-piercing riveted joint”. *Key Engineering Materials*, 344, pp. 655–662, 2007.

[9] Cuntze, R. "Facts and effects to be considered when validating 2D and 3D UD composite failure conditions – experiences from participation in the World-Wide-Failure-Exercise", *Structural Durability and Health Monitoring*, Vol. 6, No.3, 2010.